Biosensors and Bioelectronics 72 (2015) 383–392

Contents lists available at ScienceDirect

Biosensors and Bioelectronics

journal homepage: www.elsevier.com/locate/bios

Ultra-high frequency piezoelectric aptasensor for the label-free detection of cocaine

Miguel A.D. Neves [a], Christophe Blaszykowski [b], Sumra Bokhari [c], Michael Thompson [a,b,c,*]

[a] Department of Chemistry, University of Toronto, 80 St. George Street, Toronto, Ontario, Canada M5S 3H6
[b] Econous Systems Inc., 80 St. George Street, Toronto, Ontario, Canada M5S 3H6
[c] Institute for Biomaterials and Biomedical Engineering, University of Toronto, 164 College Street, Toronto, Ontario, Canada M5S 3G9

ARTICLE INFO

Article history:
Received 12 February 2015
Received in revised form
30 April 2015
Accepted 16 May 2015
Available online 17 May 2015

Keywords:
Electromagnetic piezoelectric acoustic sensor
Cocaine aptamer
Aptasensor
Biosensor
Organosilane adlayer

ABSTRACT

This paper describes a label-free and real-time piezoelectric aptasensor for the detection of cocaine. The acoustic wave sensing platform is a quartz substrate functionalized with an adlayer of *S*-(11-trichlorosilyl-undecanyl)-benzenethiosulfonate (BTS) cross-linker onto which the anti-cocaine MN4 DNA aptamer is next immobilized. Preparation of the sensor surface was monitored using X-ray photoelectron spectroscopy (XPS), while the binding of cocaine to surface-attached MN4 was evaluated using the electromagnetic piezoelectric acoustic sensor (EMPAS). The MN4 aptamer, unlike other cocaine aptamer variants, has its secondary structure preformed in the unbound state with only tertiary structure changes occurring during target binding. It is postulated that the highly sensitive EMPAS detected the binding of cocaine through target mass loading coupled to aptamer tertiary structure folding. The sensor achieved an apparent K_d of 45 ± 12 μM, and a limit of detection of 0.9 μM. Repeated regenerability of the sensor platform was also demonstrated. This work constitutes the first application of EMPAS technology in the field of aptasensors. Furthermore, it is so far one of the very few examples of a bulk acoustic wave aptasensor that is able to directly detect the binding interaction between an aptamer and a small molecule in a facile one-step protocol without the use of a complex assay or signal amplification step.

1. Introduction

Currently, medical laboratories rely on a two-tiered approach to drug-of-abuse testing, the first being a qualitative test followed by a confirmatory quantitative test (Wu et al., 2003). Quantitative tests are based on conventional chromatography[1] and spectroscopy[2] techniques. These methods are complex, time-consuming, labor-intensive and expensive. The currently practiced qualitative tests are generally immunoassay-based (Wu et al., 2003). However, immunoassays, although rapid, have limitations associated with sensitivity, cross-reactivity and high cost due to the required monoclonal antibodies. It is therefore beneficial to develop rapid, sensitive and inexpensive drug-of-abuse detection techniques for use in law enforcement and clinical diagnostics. Aptamer-based assays may provide an avenue to alleviate some of the drawbacks of current detection technologies. Aptamer–ligand interactions are often compared to their antibody–antigen counterparts. However, DNA aptamers have some key advantages over antibodies, such as a comparatively smaller size, a cheap synthesis, an *in vitro* selection process, an increased resistance to degradation, and reversible denaturation.

The development of aptamer-based sensors, or aptasensors, is a rapidly expanding area of biochemistry and detection science. Despite their aforementioned advantages, aptasensors have yet to replace conventional immunoassays in analytical and medical laboratories. Perhaps one reason for the lack of aptasensor adoption is the lack of structure conservation in comparison to that of antibodies. Most aptasensors are designed to take advantage of structural differences between the free and complexed state of aptamer receptors (Li et al., 2010; Reinstein et al., 2011; Xie and Walton, 2009). However, unlike antibodies whose structure is mostly conserved (at exception of the variable antigen-binding region) aptamer structures highly vary between different aptamers. Furthermore, many aptasensors require the aptameric probe to be chemically tagged or modified (Baker et al., 2006; Freeman et al., 2010; He et al., 2011, 2013; Shlyahovsky et al., 2007; White et al., 2008). Since there is no universal means of adding a chemical probe or tag to an aptamer, this further complicates sensor

* Corresponding author at: Department of Chemistry, University of Toronto, 80 St. George Street, Toronto, Ontario, Canada M5S 3H6. Fax: +1 416 978 8775.
E-mail address: mikethom@chem.utoronto.ca (M. Thompson).

[1] Brunetto et al. (2010), Buryakov (2004), Clauwaert et al. (1996), Strano-Rossi et al. (2005), Trachta et al. (2004).

[2] Drummond et al. (2003), Du et al. (2010), Fan et al. (2005), Oiye et al. (2009), Xiao et al. (2005).

http://dx.doi.org/10.1016/j.bios.2015.05.038
0956-5663/

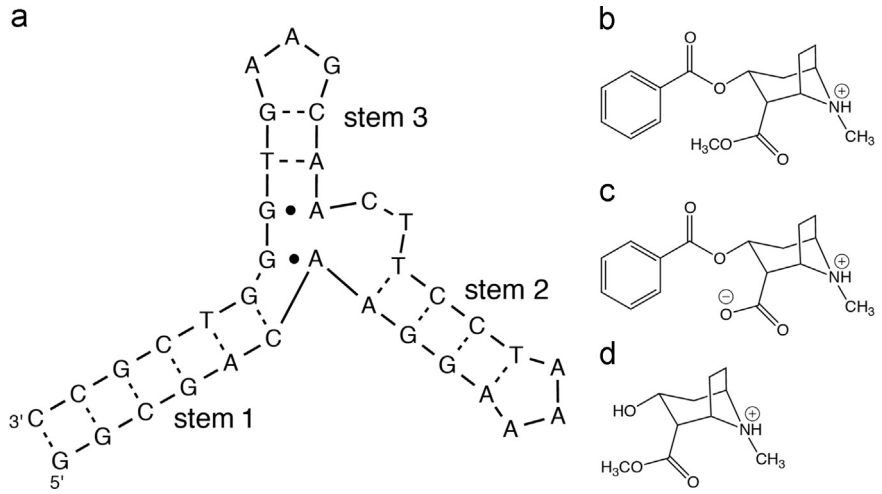

Fig. 1. (a) Secondary structure of the MN4 cocaine binding aptamer. Dashed lines between nucleotides indicate Watson–Crick base pairs, and dots represent non-Watson–Crick base pairs. Chemical structure of (b) cocaine, and its common metabolites (c) benzoyl ecgonine and (d) ecgonine methyl ester.

design as each aptamer must be studied in detail to determine which regions need to be conserved and which can be modified in order to maintain proper function.

The thickness shear mode (TSM) sensor (sometimes referred to as the quartz crystal microbalance or QCM), the most commonly employed bulk acoustic wave sensor, provides a more universal label-free sensor platform. TSM is a powerful technique that allows for the real-time detection of mass loading and viscoelastic changes at the liquid/sensor interface (Keller and Kasemo, 1998; Stavila et al., 2012). This technology has been widely implemented in the study and detection of biological interactions, primarily the detection of DNA oligos and protein; also several aptasensors against protein, DNA and cellular targets have been built on this technology (He et al., 2014; Ozalp et al., 2015; Shan et al., 2014; Song et al., 2014; Wang and Li, 2013). However, the detection of small organic molecules is rarely reported, due to the small mass and viscoelastic changes produced by the adsorption/binding of such small entities to the sensor surface (Chen et al., 2011; Dong and Zhao, 2012; Sheng et al., 2011). Generally, TSM sensors developed for small molecule detection do not directly detect the binding of the small molecule to the surface-immobilized probe but, instead, require the use of complicated competition/displacement assays or other signal amplification methodologies (Sheng et al., 2014; Shi et al., 2013; Zhang et al., 2012a).

The electromagnetic piezoelectric acoustic sensor (EMPAS) is a device developed in our laboratory (Ballantyne and Thompson, 2004; Thompson et al., 2003). Unlike other, more conventional piezoelectric sensors (i.e. TSM) excitation of acoustic resonance occurs remotely within an electrode-free piezoelectric quartz substrate through an external magnetic field generated by a spiral coil placed 30 μm underneath. This arrangement allows for the sensor to operate at ultra-high frequencies (> 1 GHz), and for interfacial phenomena to be studied in a direct manner through the avoidance of intercalated metal contacts (plated electrodes) upon which surface chemistry is carried out (Thompson et al., 2003). The coil and piezoelectric substrate are located in a sample cell, wherein a running buffer is flowed, hence the EMPAS operates in an online and real-time detection format. In practice, the sensor has been successfully applied for the detection of proteins (Sheikh et al., 2011, 2010), and lipopolysaccharide pathogens (Thompson et al., 2015), as well as for the evaluation of surface fouling (Sheikh et al., 2013, 2012). Functionalization of the EMPAS sensor platforms is generally achieved through the use of conditioning organic adlayers. These create an environment favorable to the controlled immobilization of biological probes, and are capable of resisting non-specific adsorption.

The cocaine binding DNA aptamer has become a template for use in a wide range of studies including aptamer small molecule interactions and biosensor applications. The secondary structure of the aptamer is composed of three stem loops that meet in a central three-way junction, that encompasses the cocaine binding pocket (Fig. 1a depicts the secondary structure of the MN4 cocaine aptamer variant). The aptamer has its secondary structure preformed in the absence of ligand, and it is only upon cocaine complexation that tertiary folding occurs. One reason for the widespread use of the cocaine aptamer in sensing technologies is that it can be engineered to undergo a ligand-induced folding mechanism. When stem 1 is shortened to contain three base pairs, the resulting aptamer is unfolded when free, and ligand-binding induces folding (Neves et al., 2010a,b). Another commonly used method to achieve ligand-induced folding is to divide the aptamer into two separate strands that assemble into a single tertiary complex upon cocaine binding (Stojanovic et al., 2000). The vast majority of biosensors based on the cocaine aptamer rely on one of the two ligand-induced folding variants described, rather than the rigid secondary structure variant.[3]

Herein, we describe the EMPAS as the foundation of an ultra-high frequency, label-free acoustic wave aptasensor for the detection of cocaine. The wide operating frequency range offered by the EMPAS system allows for the signal-to-noise ratio to be tuned, hence for the sensitivity of the aptasensor to be maximized. The piezoelectric sensing platform is comprised of a *S*-(11-trichlorosilyl-undecanyl)-benzenethiosulfonate (BTS) adlayer-coated quartz disc to which the cocaine binding DNA aptamer, MN4 (Fig. 1a), is immobilized (Scheme 1). This is termed the MN4 cocaine aptasensor (M4CA). Unlike the structure-switching variants that are utilized in most cocaine aptamer-based biosensors, the MN4 aptamer has its secondary structure formed in the unbound state, and no large-scale secondary structure rearrangements occur during target binding (Neves et al., 2010a,b). Furthermore, the sensitive acoustic wave EMPAS device allows for M4CA to detect the aptamer-cocaine binding interaction directly in a label-free manner using a facile, additive-free, one-step assay. This work

[3] Baker et al. (2006), Das et al. (2012), Deng et al. (2012), Du et al. (2010), Golub et al. (2009), He et al. (2010), Jiang et al. (2012), T. Li et al. (2007), Y. Li et al. (2007), Li et al. (2014, 2011), Nie et al. (2013), Sharma and Heemstra (2011), Shi et al. (2013), Smith et al. (2014), Spiropulos and Heemstra (2012), Stojanovic and Landry (2002), Stojanovic et al. (2001, 2000), White et al. (2008), Yan et al. (2013), Zhang et al. (2012b, 2008), Zhou et al. (2012, 2011), Zou et al. (2009).

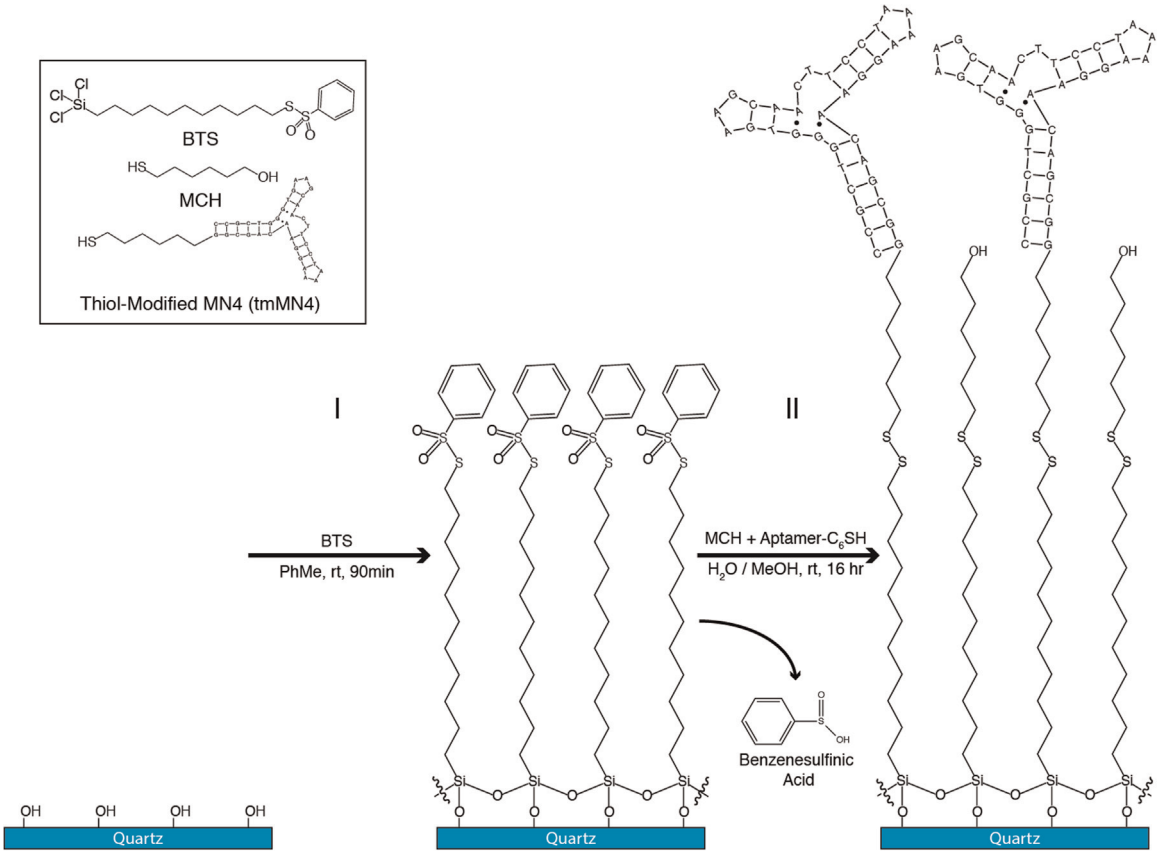

Scheme 1. Illustration of the formation of a BTS adlayer onto a cleaned piezoelectric quartz substrate (step I) and the subsequent site-specific immobilization of tmMN4 probe and MCH spacer onto the BTS precursor adlayer (step II).

constitutes not only the first application of EMPAS technology in the field of aptasensors but also, to the best of our knowledge, one of the first bulk acoustic wave label-free aptasensors that invokes the use of an aptamer immobilized onto an organic adlayer to directly detect the binding interaction between an aptamer and a small molecule.

2. Experimental

Unless otherwise specified, all reagents were purchased from Sigma-Aldrich® and used as received.

2.1. tmMN4 aptamer purification

5'-thiol-modified MN4 (tmMN4) DNA aptamer samples (aptamer–$(CH_2)_6$–S–S–$(CH_2)_6$–O–DMT) were obtained from the University of Calgary Core DNA Service (Calgary, Alberta, Canada). The DNA samples were then purified by denaturing (7 M urea) 20% polyacrylamide gel electrophoresis. The DNA was electroeluted from the gel; and the recovered DNA samples were pooled, exchanged three times with sterilized 1 M NaCl in a 3 kDa molecular mass cutoff centrifugal filter (Millipore® Amicon Ultra Centrifugal Filter), and subsequently washed three times with distilled deionized water (ddH_2O).

2.2. Quartz substrate cleaning

Quartz discs were obtained from Lap-Tech Precision Inc. (Bowmanville, Ontario, Canada) and are AT-cut, with a 13.5 mm diameter and 20.0 MHz fundamental frequency. Quartz discs were sonicated for 30 min in ~20 mL of Vayselle concentrated detergent (Dustbane Products Ltd.) diluted 50% in ddH_2O. Quartz discs were then rinsed with warm tap water followed by distilled water, and then dried under a gentle stream of forced air. Quartz discs were then individually soaked for 45 min in "piranha solution" (3/1 (v/v) mixture of concentrated H_2SO_4 and 30% H_2O_2) at 90 °C. Quartz discs were then rinsed with distilled water (× 3) followed by spectrograde methanol (× 3). Next, the discs were sonicated in spectrograde methanol for 2 min, and then individually placed in vials to be dried at 180 °C for 2 h. After drying, the discs were incubated overnight at room temperature in a humidity chamber at 80% relative humidity.

2.3. BTS silanization

The cross-linker used for adlayer formation, *S*-(11-trichlorosilyl-undecanyl)-benzenethiosulfonate (BTS), was prepared as previously described (Blaszykowski et al., 2012). To prevent any undesired reaction of trichlorosilane BTS molecules with the walls of the test tubes used during silanization, all silanization glassware was pre-treated with octadecyltrichlorosilane (1/20 (v/v) solution in anhydrous toluene). Under a nitrogen atmosphere, a 0.1% (v/v) solution of neat BTS diluted in anhydrous toluene was prepared. Cleaned quartz discs (as described above) were then individually soaked in 1 mL of BTS solution in sealed tubes, which were removed from the glovebox and incubated for 2 h at room temperature. The discs were then rinsed twice with dry toluene, sonicated in toluene for 5 min, and finally rinsed again with dry toluene. The previous rinsing procedure was repeated with dry chloroform. After a final rinse with chloroform, the discs were dried under a gentle stream of N_2 gas.

2.4. Cleavage of the thiol-protecting group from tmMN4

The day prior to aptamer immobilization, the thiol-protecting group of the purified MN4 sample was cleaved by incubating the thiol-labeled aptamer in dithiothreitol (DTT) containing deprotection buffer (20 mM borate, 100 mM DTT, pH 8.5) for 1 h. Following deprotection, the aptamer sample was dialyzed overnight into ultrapure deionized H_2O using a 2 kDa cutoff Slide-A-Lyzer® dialysis cassette (Thermo Scientific®).

2.5. Immobilization of deprotected tmMN4

BTS-silanized quartz substrates were individually submerged in 1 mL of 10 μM purified and deprotected MN4 aptamer in immobilization solvent [10 μM mercaptohexanol (MCH) dissolved in 1/1 (v/v) ddH_2O/spectrograde methanol] for 16 h. Prior to the addition of the quartz substrates, the aptamer-containing immobilization solvent was heated in a boiling water bath for 5 min, then cooled on ice to anneal the aptamer. Following the incubation time, the functionalized discs were subsequently rinsed twice with ddH_2O, sonicated for 5 min, and then finally rinsed again with a clean portion of ddH_2O. The previous ddH_2O rinsing procedure was then repeated with spectrograde methanol. The substrates were finally dried under a gentle stream of N_2 gas, and then placed into screw-cap vials in preparation for EMPAS analysis.

2.6. EMPAS cocaine binding measurements

EMPAS samples were prepared in PBS buffer (10 mM $NaHPO_3$, 138 mM NaCl, 2.7 mM KCl, pH 7.4). Upon the standard EMPAS setup procedure (Ballantyne and Thompson, 2004), each prepared disc was inserted into the EMPAS flow-cell, and PBS used as the running buffer was flowed over the sensing surface at a rate of 40 μL/min. Once the signal stabilized at the desired frequency (~860 MHz – 43rd harmonic), the 50 μL sample loop was loaded with freshly-prepared cocaine sample and injected into the flow-cell, using a low-pressure liquid chromatography valve. Once the uninterrupted PBS buffer flow carried the cocaine sample through the flow-cell, the frequency signal was allowed to restabilize. [If another injection was to be made (regeneration study), it would be made at this point.] The net frequency shift was then calculated to be the difference between the pre-injection stabilized baseline frequency and the post-injection restabilized frequency.

2.7. Determination of apparent K_d

To determine the apparent dissociation constant (K_d) of the MN4 cocaine aptasensor, cocaine solutions of 2, 10, 25, 50, 100, 250, and 400 μM were prepared in PBS buffer (10 mM $NaHPO_3$, 138 mM NaCl, 2.7 mM KCl, pH 7.4) and run on the EMPAS, in triplicate or more. The resultant frequency shifts were plotted against concentration and analyzed with the SigmaPlot® software package (Systat Software®). The data was fit to a one-site saturation ligand-binding model, Eq. (1), using a single x and replicate y data input method (B_{max} is the maximum specific binding signal).

$$y = \frac{B_{\max} x}{K_d + x} \tag{1}$$

2.8. Determination of the limit of detection

The concentration limit of detection (C_{LoD}) was determined from the residual standard deviation of the regression data obtained from the least squares regression of the linear region of the dose–response curve (Lavagnini and Magno, 2007; Miller and Miller, 2010; US Food and Drug Administration, 1996). Least squares linear regression of the linear region of the dose–response curve (2–50 μM) was performed using the SigmaPlot® software package (Systat Software®). The resultant regression parameters were then used to determine the C_{LoD} as described by Eq. (2), where m is the slope determined by least squares regression, and $s_{y/x}$ is the standard deviation of the regression residuals. The $s_{y/x}$ term is calculated from regression parameters according to Eq. (3), where $\sum (Y_i - \hat{Y}_i)^2$ is the summed squares of the regression residuals, and n is the number of replicates.

$$C_{LOD} = \frac{3S_{y/x}}{m} \tag{2}$$

$$S_{y/x} = \sqrt{\frac{\sum (y_i - \hat{y}_i)^2}{n-2}} \tag{3}$$

2.9. XPS characterization

Angle-resolved X-ray photoelectron spectroscopy (XPS) for quartz substrate silanization (adlayer formation) and subsequent MN4 immobilization was performed with a Theta probe XPS Instrument (ThermoFisher Scientific®) located at Surface Interface Ontario (University of Toronto, Toronto, Ontario, Canada). Samples were analyzed with monochromated Al Kα X-rays at take-off angles of 27.5°, 42.5°, 57.5° and 72.5° relative to the normal of the surface. The binding energy scale is calibrated to the main C_{1s} signal at 285 eV. Peak fitting and data analysis were performed with the Avantage Data System software package (ThermoFisher Scientific®) provided with the instrument. Complete XPS data are available in the accompanying supporting information.

3. Results

3.1. Sensor surface preparation and characterization

EMPAS platforms were prepared upon formation of BTS adlayers on cleaned quartz discs followed by immobilization of tmMN4 (Scheme 1). Each step of surface preparation was characterized using angle-resolved XPS following the evolution of the characteristic elements of quartz (Si and O), BTS (C and S) and tmMN4 (N), as shown in Fig. 2a. Beside the small signal attributed to unavoidable adventitious carbon contamination, bare quartz showed signals for oxygen and silicon at an approximate 2:1 ratio, as would be expected for quartz (SiO_2). Following BTS adlayer formation, signals appeared for carbon and sulfur. In contrast, the oxygen and silicon signals (that mainly originate from the now underlying quartz substrate) decreased. Upon tmMN4 aptamer immobilization, while the level of carbon further increased and those of oxygen and silicon further decreased, that of sulfur remained relatively unchanged. However, a signal appeared for nitrogen, the one element exclusively associated with tmMN4 probe. XPS sulfur narrow scans provide further evidence of tmMN4 immobilization. The sulfur narrow scan of a BTS-modified surface (Fig. 2b) reveals two distinct sulfur peaks – one centered at 164 eV, the other at 169 eV – respectively corresponding to the sulfide and sulfone moieties of BTS residues. Following treatment of the BTS-modified surface with tmMN4, the sulfone sulfur peak (169 eV) disappears corresponding to the displacement of the terminal benzenesulfonyl leaving group of BTS by tmMN4 (Scheme 1). Contact angle measurements were also taken for each step of surface preparation (Fig. 2a). Contact angle values for bare quartz, BTS adlayer and M4CA were determined to be 11°, 76° and 54°, respectively.

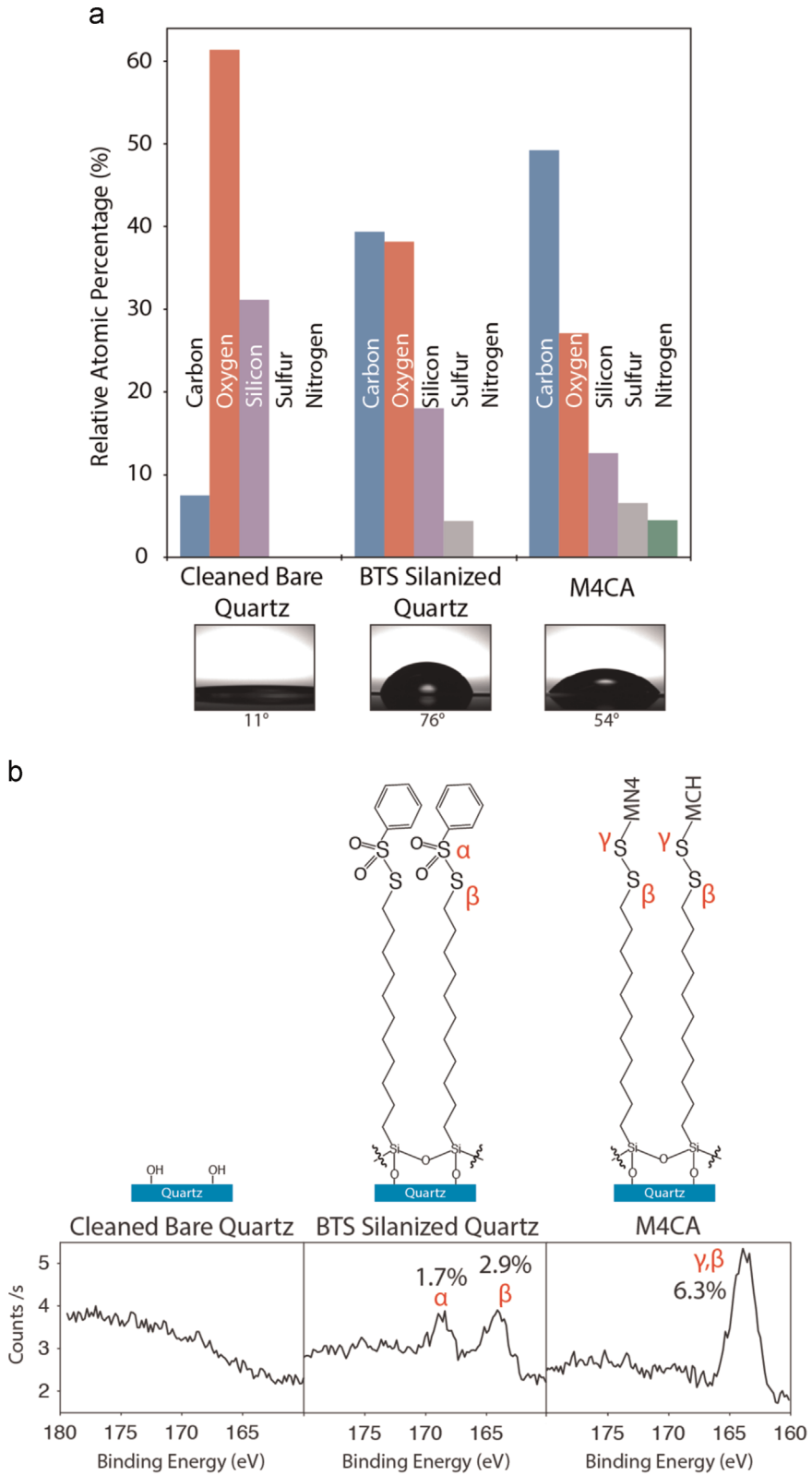

Fig. 2. (a) Summary of XPS data showing the relative atomic percentages of characteristic elements C, O, Si, S and N monitored at each stage of sensing platform preparation (the take-off angle shown here is 52.5° relative to normal). Also shown below the graph are the corresponding static contact angle images/measurements recorded with ddH_2O as the test liquid. (b) XPS sulfur narrow scans at an analysis angle of 27.5° relative to the normal, and schematic representation of the surface of cleaned bare quartz, BTS-only silanized quartz, and the EMPAS cocaine aptasensor. The symbols α, β and γ respectively correspond to the BTS sulfone, the BTS sulfide, and the sulfide from immobilized tmMN4/MCH. Relative atomic percentage values are indicated next to the corresponding XPS sulfur peaks.

3.2. Target interaction

Substrates at each phase of the manufacturing process were analyzed with the EMPAS system. Each surface was contacted with 100 μM cocaine in PBS with the EMPAS operating at the ultra-high resonant frequency of 860 MHz. When exposed to 100 μM cocaine,

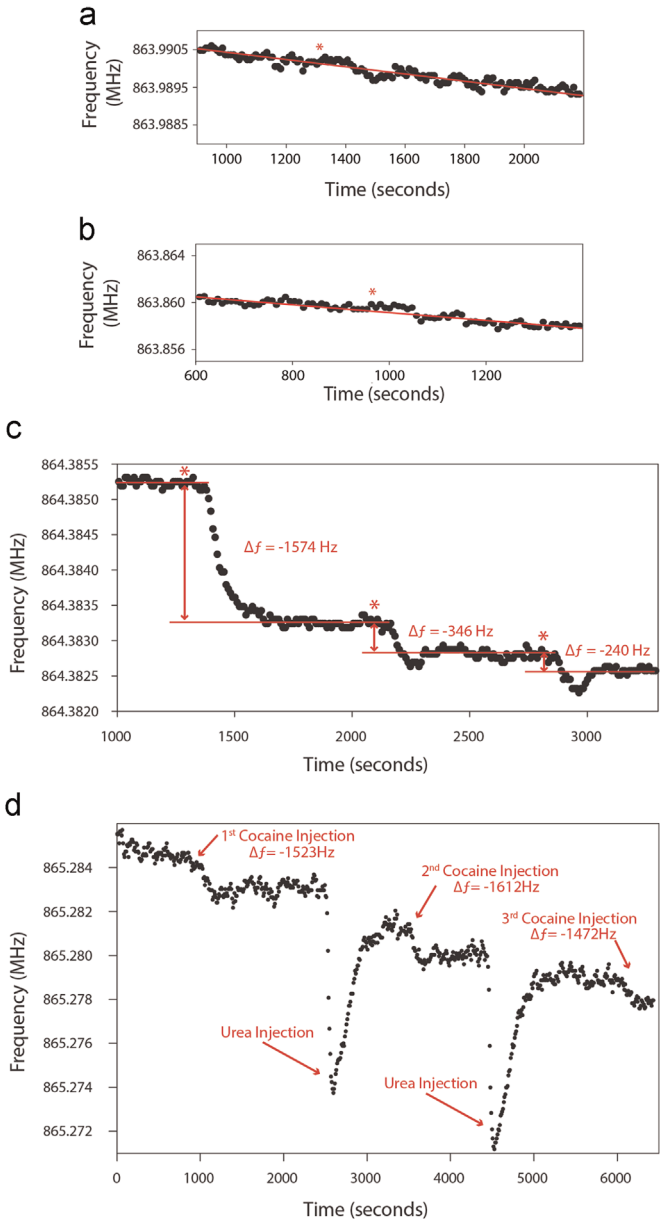

Fig. 3. Typical EMPAS responses to injections of 100 μM cocaine in PBS contacting (a) a BTS-only silanized quartz substrate, (b) a MCH-only functionalized BTS adlayer-coated quartz substrate, and (c) the EMPAS cocaine aptasensor. Cocaine injections are denoted by *. (a) and (b) produce no detectable response, whereas (c) produces three frequency shifts following the three cocaine injections. The first frequency shift is large followed by two smaller frequency shifts, indicating near-saturation of the sensor surface after the first injection. (d) Three successive injections of 100 μM cocaine in PBS, followed by that of 7 M urea, highlight the repeated regeneration of the binding capability of the M4CA platform.

no EMPAS response was detected for cleaned, bare quartz substrates and BTS-only silanized surfaces (Fig. 3a). However, M4CA platforms generated an EMPAS frequency shift of -1648 ± 260 Hz when contacted with 100 μM cocaine [representative response shown in Fig. 3c (first injection)]. To verify whether the signal was due to the interaction between cocaine and the surface-bound aptamer, and not due to any interaction with MCH spacing residues, a MCH-only functionalized BTS adlayer-coated quartz surface was produced. Upon contact with 100 μM cocaine, the MCH-functionalized surface did not produce any detectable frequency shift (Fig. 3b). To further test whether cocaine interacts non-specifically with the sensing platform, cleaned bare quartz, as well as non-functionalized and MCH-functionalized BTS adlayer surfaces were contacted with 400 μM cocaine. All three surfaces showed no affinity for the target analyte (data not shown).

Once cocaine enters the body, it is quickly metabolized into the major metabolites benzoylecgonine (BE) and ecgonine methyl ester (EME) (Kolbrich et al., 2006), the chemical structures of which can be seen in Fig. 1c and d. To evaluate the selectivity of the EMPAS cocaine aptasensor towards cocaine, the sensing platform was also individually contacted with 100 μM of BE, and 100 μM of EME. Upon injection, the EMPAS produced no detectable response to either metabolite (Table S2).

3.3. Reusability of the M4CA sensing platform

The reusability of M4CA was tested by sequential injections of 100 μM cocaine over a same platform, as shown in Fig. 3c. It can be seen that the initial cocaine injection caused a frequency shift of −1574 Hz; however, the two subsequent cocaine injections only garnered a response of −346 and −240 Hz, respectively. The result demonstrates that the target analyte had almost completely saturated the M4CA sensor surface after the first injection as the subsequent injections generated very small frequency shifts. It was then decided to denature the surface-bound aptamer with 7 M urea in order to release bound cocaine between injections. The M4CA reusability experiment consisted of three repeated injections of 100 μM cocaine, each being followed by an injection of 7 M urea. The course of the experiment is shown in Fig. 3d. Here, it can be seen that the initial cocaine injection produced a shift of −1523 Hz. Following the (first) introduction of 7 M urea, the second cocaine injection produced a shift of −1612 Hz. After a second urea-denaturing step, a shift of −1472 Hz was observed after the third and final cocaine injection. Injection of urea over the cocaine-bound MN4-coated platform produces large frequency shifts that nearly revert back to the original, pre-injection baseline.

3.4. Analytical performance of M4CA

M4CA was contacted with a series of cocaine concentrations ranging from 2 to 400 μM (data tabulated within Table S2). A clear decrease in EMPAS frequency was recorded upon injection of each cocaine solution. Fig. 4a shows representative frequency shifts at each concentration. The observed frequency shifts increased along with cocaine concentration until 100 μM at which point changes in signal were very small. Frequency shifts were plotted against cocaine concentration to obtain the binding curve shown in Fig. 4b. The apparent dissociation constant (K_d) was determined to be 45 ± 12 μM by fitting the data to a one-site saturation ligand-binding model. Analysis of the binding curve revealed a relatively small dynamic range from 2 to 50 μM. The dynamic range frequency shifts were plotted against concentration and fit to a least squares linear regression. The regression parameters were used to determine the concentration limit of detection (C_{LoD}). The latter was determined to be C_{LoD}=0.9 μM.

4. Discussion

4.1. Sensor surface preparation

Our strategy involved the preparation of robust and functionalizable surfaces upon EMPAS quartz discs using the BTS surface modifier, as shown in Scheme 1. The BTS cross-linking molecule possesses a highly reactive trichlorosilyl tail function, for strong siloxane attachment onto the quartz substrates. The distal benzenethiosulfonate head function readily and regioselectively reacts with thiols to form disulfide bridges (Chan et al., 2013; Sheikh

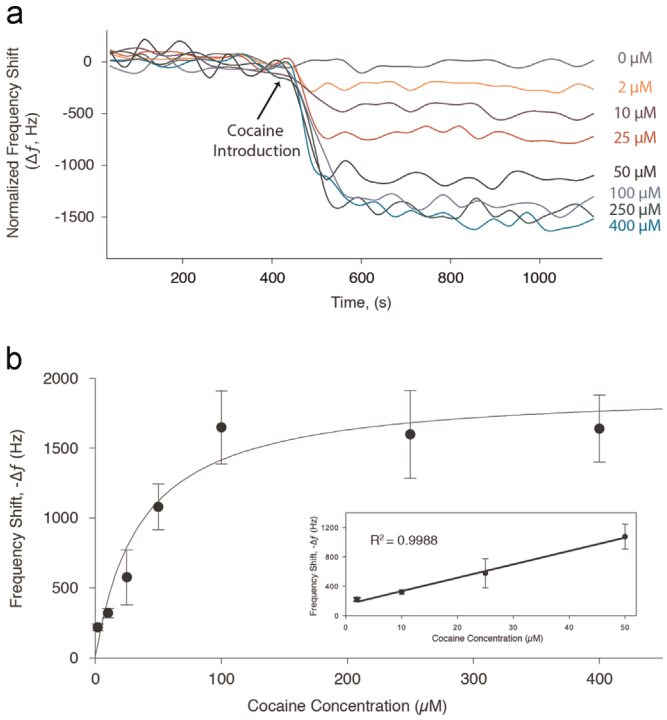

Fig. 4. (a) Representative EMPAS frequency shifts of the MN4 cocaine aptasensor at different cocaine concentrations. (b) The dose–response curve for MN4-immobilized aptasensor platforms exposed to a wide range of cocaine concentrations. EMPAS frequency response is plotted against cocaine concentration, and then fitted to a ligand-binding curve. The resulting apparent dissociation constant (K_d) is calculated to be 45 ± 12 μM. The inset plot shows the linear region of the dose–response curve used to determine the concentration limit of detection, which was calculated to be 0.9 μM. Each point represents the average of a minimum of three independent experiments, and the error bars are the corresponding standard deviations.

et al., 2010). BTS has recently been used as a surface modifier on both medical grade stainless steel and aluminum nitride to facilitate the functionalization of those surfaces with thiol-containing probes (Blaszykowski et al., 2012; Chan et al., 2013). The tmMN4 aptamer was next concurrently immobilized with MCH spacer molecule onto BTS-modified surfaces, at a 1:1 M ratio in the immobilization solution. The purpose of the MCH is to space out the MN4 aptamer on the BTS surface in order to alleviate possible steric hindrance between otherwise tightly-packed neighboring aptamers residues. This, in turn, would be expected to increase the affinity of surface-bound MN4 towards cocaine.

Upon BTS silanization of the quartz substrates, XPS data displays a large atomic percentage for carbon, as well as the presence of a signal for sulfur – the only element exclusively found in the BTS cross-linking residues. Conversely, a reduction in the atomic percentage of both silicon and oxygen was observed. This is a clear indication of a carbon-rich, sulfur-containing adsorbed BTS film that attenuates the silicon and oxygen signals of the underlying quartz substrate. Following tmMN4 immobilization, there was further reduction of both oxygen and silicon signals, and a minimal change in the atomic percentage of sulfur. However, the data clearly displays an increase in the carbon signal and the appearance of nitrogen – an element solely associated with tmMN4 – indicating successful immobilization of the MN4 aptamer onto the BTS adlayer.

When the BTS head function reacts with a thiol-containing species, the terminal benzenesulfonyl moiety is displaced by the incoming thiol function producing benzenesulfinic acid in the process (Scheme 1). This reaction can be probed following the evolution of the XPS sulfur narrow scans. The BTS-silanized surface produced two sulfur peaks, one corresponding to the sulfone (169 eV) and the other to the sulfide (164 eV) moieties of BTS. Following tmMN4 immobilization, only the sulfide peak remained corresponding to the formation of a di-sulfide between tmMN4 and BTS cross-linking residues. The complete disappearance of the sulfone peak is likely due to the co-immobilization of tmMN4 and MCH spacer. Considering its relative size, if tmMN4 were solely immobilized onto the BTS film, there likely would be too much steric hindrance for tmMN4 to react with every available BTS head functions. Therefore, the resulting single sulfide peak most likely arises from a mixture of covalently-bound tmMN4 receptors and MCH spacing residues.

4.2. Sensor performance

The initial experiments of the EMPAS cocaine aptasensor were promising. The completed device showed affinity for the target analyte producing a shift of -1648 ± 260 Hz when exposed to 100 μM cocaine. When contacted with the common cocaine metabolites (BE and EME – Fig. 1), the device produced no discernible response. This observed selectivity of the sensor towards cocaine over its metabolites was not an unexpected result as an initial fluorescent aptasensor based on a structure-switching aptamer variant displayed very high selectivity for cocaine over its metabolites (Stojanovic et al., 2001). Furthermore, the quartz substrate was contacted with 100 and 400 μM cocaine at each stage of the sensing platform manufacturing process. The data shows that the cleaned quartz surface and the BTS-only silanized surface display no affinity towards the target. Also, BTS-silanized surfaces functionalized with just the MCH spacer were prepared and contacted with 100 and 400 μM cocaine. Results (Fig. 3b) indicated that areas covered by/filled with MCH spacer prevent cocaine non-specific adsorption.

Cocaine sensors based on a shortened stem 1 construct of the cocaine aptamer have been shown to regenerate binding ability by flowing or rinsing the sensing surface with running buffer (Baker et al., 2006). However, as Fig. 3c shows, flowing running buffer over the M4CA sensor platform after a cocaine injection does not cause MN4 to release its target. Instead, the cocaine binding ability of the sensor was regenerated by introducing the chaotropic agent urea. Fig. 3d follows the course of an EMPAS experiment, where the sensor is regenerated by injection of 7 M urea denaturant between each 100 μM cocaine injection. The standard deviation between the three cocaine injections of the regeneration experiment (Fig. 3d) is ± 71 Hz or ~4.5%. This is better than the ± 260 Hz or ~16% standard deviation seen between replicate experiments (batch variance), a larger discrepancy most likely due to the sensing platform manufacturing process.

Cocaine concentrations varying from 2 to 400 μM were contacted with M4CA. A cocaine dose–sensor response curve was plotted and the data fitted to a one-site binding model. The apparent K_d of the sensor was determined to be 45 ± 12 μM. The sensor also displayed a relatively small linear range from 2 to 50 μM. The literature cites dissociation constants for variants of the cocaine aptamer ranging between 1 and 150 μM – depending on the aptamer variant, reaction buffer, and analysis technique (sensor) used. Detection methods with the aptamer dissolved in solution generally produce a K_d in the 1–20 μM range (Baker et al., 2006; Cekan et al., 2009; Chen et al., 2008; Neves et al., 2010a,b; Stojanovic et al., 2001; White et al., 2008). The detection limit of M4CA was calculated to be 0.9 μM, importantly this value falls within the US Government Substance Abuse & Mental Health Services Administration's cocaine initial drug test cut-off level (300 ng/mL or 1 μM for the qualitative initial test, and 150 ng/mL or 0.5 μM for the quantitative confirmatory test) (Wen et al., 2011). Even though M4CA falls just short of the confirmatory test

Table 1
Comparison of the analytical performance of other cocaine aptamer-based assays without a signal amplification step.

Detection method	Strategy	C_{LoD} (μM)	Limitation(s)
Colorimetric	Split aptamer ligation in the presence of AuNPs (SA) (TB) (Zhang et al., 2008)	2	Sample must be doped with the split aptamer strands and AuNPs
	Aptamer immobilized onto micro-cantilever sensor surface (RA) (PB) (Kang et al., 2011)	5	Does not meet both the US government qualitative and confirmatory testing guidelines
Electrochemical	Microfluidic microchip embedded biological nanopore (SS1) (PB) (Kawano et al., 2011)	1	Sample doped with split aptamer strand
	Cocaine-induced split aptamer self-assembly on electrode surface (SA) (PB) (Zuo et al., 2009)	1	Sample doped with methylene blue-labeled split aptamer strand
	Microfluidic electrochemical aptamer-based sensor (SS1) (BS) (Swensen et al., 2009)	10	Aptamer labeled with methylene blue
Capillary electrophoresis	Capillary electrophoresis of split aptamer (SA) (PB) (Deng et al., 2012)	5	Carboxyfluorescein-labeled aptamer
Fluorescence	Aptamer hybridized to AuNP-immobilized oligo. Upon binding cocaine the AuNP is no longer able to quench the aptamer attached fluorescent tag (RA) (TB) (Ge et al., 2012)	2.1	Aptamer labeled with a fluorescent tag
	Aptamer folding-based FRET (SS1) (TB) (Stojanovic et al., 2001)	10	Aptamer labeled with fluorescein and a quencher
Surface Plasmon Resonance	Cocaine-induced assembly of AuNP-aptamer subunits (SA) (PB) (Golub et al., 2009)	1	Sample doped with AuNP-labeled split aptamer strand
EMPAS (this work)	MN4 immobilized onto piezoelectric surface, the added mass and tertiary structure rearrangement cause observed signal (RA) (PB)	0.9	Falls short of the US government confirmatory testing guidelines

(SS1) – indicates the use of the short stem 1 cocaine aptamer variant,
(SA) – indicates the use of a split (2 stranded) cocaine aptamer variant,
(RA) – indicates use of a rigid, non-structure switching cocaine aptamer variant,
(PB) – indicates assay performed in PBS buffer,
(TB) – indicates assay performed in TRIS buffer,
(BS) – indicates assay perfumed in bovine serum

guidelines, we feel that further optimization of our assay should allow for such a cut-off level to be readily achieved. At the present time however, this aptasensor prototype may be more suited as an initial screening or qualitative technique due to its narrow dynamic range, high-throughput flow-through configuration, regenerable binding capability, and label-free operation.

Cocaine aptamer-based aptasensors have been reported that produce lower detection sensitivity than M4CA; however, these require the use of a signal amplification step (Sheng et al., 2014; Shi et al., 2013; Zhang et al., 2012a). M4CA operates in a one-step assay format in which complexation of MN4 with cocaine on the piezoelectric resonator is sufficient to generate real-time signaling, and does not require the use of label, an additive added to the analyte sample, a reporter molecule, a signal amplification step, or a combination thereof. Therefore, a comparison of sensors that do not require a signal amplification step would be more appropriate. When compared against aptamer-based aptasensors that do not rely on a signal amplification step, M4CA compares quite favorably, as seen in Table 1. Furthermore, all but one of the other aptasensors listed within Table 1 rely on a structure-switching cocaine aptamer variant to produce signals, while M4CA is able to detect cocaine more sensitively without the need for an aptameric probe that undergoes an unstructured to structured binding transition. To date, and to our knowledge, no bulk acoustic wave (BAW) biosensor using a cocaine aptamer variant as the biomolecular probe has been reported. Furthermore, this work constitutes one of the first bulk acoustic wave label-free aptasensor that invokes the use of an aptamer immobilized onto an organic adlayer to directly detect the binding interaction of a small molecule. To date, multiple literature searches have only yielded one other example of a small molecule aptasensor in which the aptameric probe immobilized onto a BAW sensor surface is capable of detecting the binding event in a label-free, one-step assay. The sensor is based on biotin-tagged adenosine triphosphate (ATP) aptamers that are immobilized onto an adsorbed streptavidin layer (Ozalp, 2011). Unlike the cocaine aptamer however, the ATP aptamer binds two ATP molecules per aptamer. Furthermore, the adsorbed streptavidin layer is not covalently-bound to the sensor surface and does not allow for the aptameric probes to be oriented on the surface of the device. The ATP aptasensor yields a similar apparent K_d (49 ± 8 μM) to that of M4CA however, the limit of detection is not reported.

A common thought is that BAW sensor signal only originates from the capture of analyte upon the device surface increasing the acoustic thickness of the surface layer, which results in an extension of the effective wavelength and a decrease in the resonant frequency (Sauerbrey, 1959; Wang et al., 2006). However, a growing body of BAW sensors presented in the literature outline instances, where the observed sensor response arises from the structural rearrangement of biomolecular probes immobilized on the sensing surface (Feiler et al., 2007; Lee et al., 2010; Thompson et al., 2015; Wang et al., 2006). In the case in point, we postulate that the signal observed for the M4CA platform is due to a combination of both the added mass of the cocaine analyte coupled to the tertiary structure rearrangement of MN4 aptamer upon cocaine binding. The mass increase due to cocaine complexation is indeed likely not sufficient to account for the entirety of the large resonant frequency shifts observed. Also, even larger frequency shifts are observed during sensor regeneration when 7 M urea is injected over the sensor platform (Fig. 3d). Contact of the sensing surface with urea causes a large drop in frequency approximately 4.5 times greater than the cocaine binding resonant frequency shift. The large frequency response likely corresponds to structural/conformation changes occurring during the denaturation and re-folding of the MN4 aptamer. A study on the effect of aptamer structural changes on EMPAS response is in progress.

5. Concluding remarks

In this study, we have developed a simple, label-free, real-time, and reusable aptasensor for the detection of cocaine. This work constitutes the first application of a BTS cross-linker for the surface modification/functionalization (with MN4 aptamer) of quartz substrates. The sensitive EMPAS system in conjunction with the M4CA platform displayed excellent selectivity to the target over its common metabolites. The aptasensor was shown to be able to

reliably bind cocaine with an apparent K_d comparable to other cocaine detection techniques also based on the cocaine aptamer. The concentration limit of detection was found to be within the qualitative testing guidelines set by the US Government Substance Abuse & Mental Health Services Administration. Also, the value is comparable to other cocaine aptamer-derived sensors that do not rely on a signal amplification step.

To our knowledge, the work presented herein constitutes one of the first examples of an aptasensor that relies on a piezoelectric resonator in conjunction with an aptamer immobilized onto an organic thin film (adlayer). We postulated that the signal observed is the result of cocaine mass loading coupled to conformational changes experienced by the platform-bound aptamer upon cocaine ligand-binding. With further optimization of both surface treatment and aptamer variant, it should be possible to increase the analytical performance of the aptasensor and allow for more complex matrices to be analyzed, that is allow for cocaine detection to be performed in real-world (e.g. urine) biosamples. This proof-of-concept work is a strong first step into the development of a universal biosensor that could be adapted to almost any molecule, as aptamers can in principle be engineered for any desired target through selection procedures such as SELEX. Furthermore, the work presented herein clearly demonstrates that the immobilized aptamer probe does not need to be structure-switching upon analyte binding for EMPAS signal to be generated.

6. Notes

The authors declare no competing financial interest.

Acknowledgments

We thank Pasquale Benvenuto (University of Toronto, Toronto, Ontario) for useful discussion and help with XPS data fitting. We also thank Dr. Alexander D. Romaschin (St. Michael's Hospital, Toronto, Ontario) for much useful discussion and use of his facilities. The authors are grateful to the Natural Sciences and Engineering Research Council of Canada (Grant No. CHRPJ413720-12) for support of this work.

Appendix A. Supplementary material

Supplementary data associated with this article can be found in the online version at http://dx.doi.org/10.1016/j.bios.2015.05.038.

References

Baker, B.R., Lai, R.Y., Wood, M.S., Doctor, E.H., Heeger, A.J., Plaxco, K.W., 2006. An electronic, aptamer-based small-molecule sensor for the rapid, label-free detection of cocaine in adulterated samples and biological fluids. J. Am. Chem. Soc. 128, 3138–3139.

Ballantyne, S.M., Thompson, M., 2004. Superior analytical sensitivity of electromagnetic excitation compared to contact electrode instigation of transverse acoustic waves. Analyst 129, 219–224.

Blaszykowski, C., Sheikh, S., Benvenuto, P., Thompson, M., 2012. New functionalizable alkyltrichlorosilane surface modifiers for biosensor and biomedical applications. Langmuir 28, 2318–2322.

Brunetto, M., del, R., Delgado, Y., Clavijo, S., Contreras, Y., Torres, D., Ayala, C., Gallignani, M., Forteza, R., Cerdà Martin, V., 2010. Analysis of cocaine and benzoylecgonine in urine by using multisyringe flow injection analysis-gas chromatography-mass spectrometry system. J. Sep. Sci. 33, 1779–1786.

Buryakov, I.A., 2004. Express analysis of explosives, chemical warfare agents and drugs with multicapillary column gas chromatography and ion mobility increment spectrometry. J. Chromatogr. B. Anal. Technol. Biomed. Life Sci. 800, 75–82.

Cekan, P., Jonsson, E.O., Sigurdsson, S.T., 2009. Folding of the cocaine aptamer studied by EPR and fluorescence spectroscopies using the bifunctional spectroscopic probe Ç. Nucleic Acids Res. 37, 3990–3995.

Chan, E., Jackson, N., Mathewson, A., Galvin, P., Alamin Dow, A.B., Kherani, N.P., Blaszykowski, C., Thompson, M., 2013. Surface modification of piezoelectric aluminum nitride with functionalizable organosilane adlayers. Appl. Surf. Sci. 282, 709–713.

Chen, J., Jiang, J., Gao, X., Liu, G., Shen, G., Yu, R., 2008. A new aptameric biosensor for cocaine based on surface-enhanced raman scattering spectroscopy. Chem. Eur. J. 14, 8374–8382.

Chen, Q., Wu, X., Wang, D., Tang, W., Li, N., Liu, F., 2011. Oligonucleotide-functionalized gold nanoparticles-enhanced QCM-D sensor for mercury(ii) ions with high sensitivity and tunable dynamic range. Analyst 136, 2572.

Clauwaert, K.M., Van Bocxlaer, J.F., Lambert, W.E., De Leenheer, A.P., 1996. Analysis of cocaine, benzoylecgonine, and cocaethylene in urine by HPLC with diode array detection. Anal. Chem. 68, 3021–3028.

Das, J., Cederquist, K.B., Zaragoza, A.A., Lee, P.E., Sargent, E.H., Kelley, S.O., 2012. An ultrasensitive universal detector based on neutralizer displacement. Nat. Chem. 4, 642–648.

Deng, Q.-P., Tie, C., Zhou, Y.-L., Zhang, X.-X., 2012. Cocaine detection by structure-switch aptamer-based capillary zone electrophoresis. Electrophoresis 33, 1465–1470.

Dong, Z.-M., Zhao, G.-C., 2012. Quartz crystal microbalance aptasensor for sensitive detection of mercury(II) based on signal amplification with gold nanoparticles. Sensors 12, 7080–7094.

Drummond, T.G., Hill, M.G., Barton, J.K., 2003. Electrochemical DNA sensors. Nat. Biotechnol. 21, 1192–1199.

Du, Y., Chen, C., Yin, J., Li, B., Zhou, M., Dong, S., Wang, E., 2010. Solid-state probe based electrochemical aptasensor for cocaine: a potentially convenient, sensitive, repeatable, and integrated sensing platform for drugs. Anal. Chem. 82, 1556–1563.

Fan, C., Plaxco, K.W., Heeger, A.J., 2005. Biosensors based on binding-modulated donor-acceptor distances. Trends Biotechnol. 23, 186–192.

Feiler, A.A., Sahlholm, A., Sandberg, T., Caldwell, K.D., 2007. Adsorption and viscoelastic properties of fractionated mucin (BSM) and bovine serum albumin (BSA) studied with quartz crystal microbalance (QCM-D). J. Colloid Interface Sci. 315, 475–481.

Freeman, R., Sharon, E., Teller, C., Willner, I., 2010. Control of biocatalytic transformations by programmed DNA assemblies. Chemistry 16, 3690–3698.

Ge, J., Liu, Z., Zhao, X.S., 2012. Cocaine detection in blood serum using aptamer biosensor on gold nanoparticles and progressive dilution. Chin. J. Chem. 30, 2023–2028.

Golub, E., Pelossof, G., Freeman, R., Zhang, H., Willner, I., 2009. Electrochemical, photoelectrochemical, and surface plasmon resonance detection of cocaine using supramolecular aptamer complexes and metallic or semiconductor nanoparticles. Anal. Chem. 81, 9291–9298.

He, J.-L., Wu, Z.-S., Zhou, H., Wang, H.-Q., Jiang, J.-H., Shen, G.-L., Yu, R.-Q., 2010. Fluorescence aptameric sensor for strand displacement amplification detection of cocaine. Anal. Chem. 82, 1358–1364.

He, J.-L., Yang, Y.-F., Shen, G.-L., Yu, R.-Q., 2011. Electrochemical aptameric sensor based on the Klenow fragment polymerase reaction for cocaine detection. Biosens. Bioelectron. 26, 4222–4226.

He, P., Liu, L., Qiao, W., Zhang, S., 2014. Ultrasensitive detection of thrombin using surface plasmon resonance and quartz crystal microbalance sensors by aptamer-based rolling circle amplification and nanoparticle signal enhancement. Chem. Commun. 50, 1481–1484.

He, X., Wang, G., Xu, G., Zhu, Y., Chen, L., Zhang, X., 2013. A simple, fast, and sensitive assay for the detection of DNA, thrombin, and adenosine triphosphate based on Dual-Hairpin DNA structure. Langmuir 29, 14328–14334.

Jiang, B., Wang, M., Chen, Y., Xie, J., Xiang, Y., 2012. Highly sensitive electrochemical detection of cocaine on graphene/AuNP modified electrode via catalytic redox-recycling amplification. Biosens. Bioelectron. 32, 305–308.

Kang, K., Sachan, A., Nilsen-Hamilton, M., Shrotriya, P., 2011. Aptamer functionalized microcantilever sensors for cocaine detection. Langmuir 27, 14696–14702.

Kawano, R., Osaki, T., Sasaki, H., Takinoue, M., Yoshizawa, S., Takeuchi, S., 2011. Rapid detection of a cocaine-binding aptamer using biological nanopores on a chip. J. Am. Chem. Soc. 133, 8474–8477.

Keller, C.A., Kasemo, B., 1998. Surface specific kinetics of lipid vesicle adsorption measured with a quartz crystal microbalance. Biophys. J. 75, 1397–1402.

Kolbrich, E.A., Barnes, A.J., Gorelick, D.A., Boyd, S.J., Cone, E.J., Huestis, M.A., 2006. Major and minor metabolites of cocaine in human plasma following controlled subcutaneous cocaine administration. J. Anal. Toxicol. 30, 501–510.

Lavagnini, I., Magno, F., 2007. A statistical overview on univariate calibration, inverse regression, and detection limits: application to gas chromatography/mass spectrometry technique. Mass Spectrom. Rev. 26, 1–18.

Lee, H.-S., Contarino, M., Umashankara, M., Schön, A., Freire, E., Smith, A.B., Chaiken, I.M., Penn, L.S., 2010. Use of the quartz crystal microbalance to monitor ligand-induced conformational rearrangements in HIV-1 envelope protein gp120. Anal. Bioanal. Chem. 396, 1143–1152.

Li, D., Song, S., Fan, C., 2010. Target-responsive structural switching for nucleic acid-based sensors. Acc. Chem. Res. 43, 631–641.

Li, T., Li, B., Dong, S., 2007. Adaptive recognition of small molecules by nucleic acid aptamers through a label-free approach. Chem. Eur. J. 13, 6718–6723.

Li, Y., Ji, X., Liu, B., 2011. Chemiluminescence aptasensor for cocaine based on double-functionalized gold nanoprobes and functionalized magnetic microbeads. Anal. Bioanal. Chem. 401, 213–219.

Li, Y., Qi, H., Peng, Y., Yang, J., Zhang, C., 2007. Electrogenerated chemiluminescence

aptamer-based biosensor for the determination of cocaine. Electrochem. Commun. 9, 2571–2575.
Li, Y., Zeng, Y., Mao, Y., Lei, C., Zhang, S., 2014. Proximity-dependent isothermal cycle amplification for small-molecule detection based on surface enhanced Raman scattering. Biosens. Bioelectron. 51, 304–309.
Miller, J.N., Miller, J.C., 2010. Statistics and Chemometrics for Analytical Chemistry. In: sixth ed. (Ed.), Technometrics. Pearson Education Limited, Harlow, UK.
Neves, M.A.D., Reinstein, O., Johnson, P.E., 2010a. Defining a stem length-dependent binding mechanism for the cocaine-binding aptamer. A combined NMR and calorimetry study. Biochemistry 49, 8478–8487.
Neves, M.A.D., Reinstein, O., Saad, M., Johnson, P.E., 2010b. Defining the secondary structural requirements of a cocaine-binding aptamer by a thermodynamic and mutation study. Biophys. Chem. 153, 9–16.
Nie, J., Deng, Y., Deng, Q.-P., Zhang, D.-W., Zhou, Y.-L., Zhang, X.-X., 2013. A self-assemble aptamer fragment/target complex based high-throughput colorimetric aptasensor using enzyme linked aptamer assay. Talanta 106, 309–314.
Oiye, E.N., Figueiredo, N.B., de Andrade, J.F., de Tristão, H.M., de Oliveira, M.F., 2009. Voltammetric determination of cocaine in confiscated samples using a cobalt hexacyanoferrate film-modifiedelectrode. Forensic Sci. Int. 192, 94–97.
Ozalp, V.C., 2011. Acoustic quantification of ATP using a quartz crystal microbalance with dissipation. Analyst 136, 5046–5050.
Ozalp, V.C., Bayramoglu, G., Erdem, Z., Arica, M.Y., 2015. Pathogen detection in complex samples by quartz crystal microbalance sensor coupled to aptamer functionalized core–shell type magnetic separation. Anal. Chim. Acta 853, 533–540.
Reinstein, O., Neves, M.A.D., Saad, M., Boodram, S.N., Lombardo, S., Beckham, S.A., Brouwer, J., Audette, G.F., Groves, P., Wilce, M.C.J., Johnson, P.E., 2011. Engineering a structure switching mechanism into a steroid-binding aptamer and hydrodynamic analysis of the ligand binding mechanism. Biochemistry 50, 9368–9376.
Sauerbrey, G., 1959. Verwendung von Schwingquarzen zur Wägung dünner Schichten und zur Mikrowägung. Z. Phys. 155, 206–222.
Shan, W., Pan, Y., Fang, H., Guo, M., Nie, Z., Huang, Y., Yao, S., 2014. An aptamer-based quartz crystal microbalance biosensor for sensitive and selective detection of leukemia cells using silver-enhanced gold nanoparticle label. Talanta 126, 130–135.
Sharma, A.K., Heemstra, J.M., 2011. Small-molecule-dependent split aptamer ligation. J. Am. Chem. Soc. 133, 12426–12429.
Sheikh, S., Blaszykowski, C., Thompson, M., 2011. Label-free detection of HIV-2 antibodies in serum with an ultra-high frequency acoustic wave sensor. Talanta 85, 816–819.
Sheikh, S., Blaszykowski, C., Thompson, M., 2013. Sacrificial BSA to block non-specific adsorption on organosilane adlayers in ultra-high frequency acoustic wave sensing. Surf. Interface Anal. 45, 1781–1784.
Sheikh, S., Sheng, J.C.-C., Blaszykowski, C., Thompson, M., 2010. New oligoethylene glycol linkers for the surface modification of an ultra-high frequency acoustic wave biosensor. Chem. Sci. 1, 271–275.
Sheikh, S., Yang, D.Y., Blaszykowski, C., Thompson, M., 2012. Single ether group in a glycol-based ultra-thin layer prevents surface fouling from undiluted serum. Chem. Commun. 48, 1305–1307.
Sheng, Q., Liu, R., Zhang, S., Zheng, J., 2014. Ultrasensitive electrochemical cocaine biosensor based on reversible DNA nanostructure. Biosens. Bioelectron. 51, 191–194.
Sheng, Z., Han, J., Zhang, J., Zhao, H., Jiang, L., 2011. Method for detection of Hg2+ based on the specific thymine–Hg^{2+}–thymine interaction in the DNA hybridization on the surface of quartz crystal microbalance. Colloids Surf. B. Biointerfaces 87, 289–292.
Shi, Y., Dai, H., Sun, Y., Hu, J., Ni, P., Li, Z., 2013. Fluorescent sensing of cocaine based on a structure switching aptamer, gold nanoparticles and graphene oxide. Analyst 138, 7152–7156.
Shlyahovsky, B., Li, D., Weizmann, Y., Nowarski, R., Kotler, M., Willner, I., 2007. Spotlighting of cocaine by an autonomous aptamer-based machine. J. Am. Chem. Soc. 129, 3814–3815.
Smith, J.E., Griffin, D.K., Leny, J.K., Hagen, J.A., Chávez, J.L., Kelley-Loughnane, N., 2014. Colorimetric detection with aptamer-gold nanoparticle conjugates coupled to an android-based color analysis application for use in the field. Talanta 121, 247–255.
Song, W., Zhu, Z., Mao, Y., Zhang, S., 2014. A sensitive quartz crystal microbalance assay of adenosine triphosphate via DNAzyme-activated and aptamer-based target-triggering circular amplification. Biosens. Bioelectron. 53, 288–294.
Spiropulos, N.G., Heemstra, J.M., 2012. Templating effect in DNA proximity ligation enables use of non-bioorthogonal chemistry in biological fluids. Artif. DNA PNA XNA 3, 123–128.
Stavila, V., Volponi, J., Katzenmeyer, A.M., Dixon, M.C., Allendorf, M.D., 2012. Kinetics and mechanism of metal–organic framework thin film growth: systematic investigation of HKUST-1 deposition on QCM electrodes. Chem. Sci. 3, 1531.
Stojanovic, M.N., de Prada, P., Landry, D.W., 2000. Fluorescent sensors based on aptamer self-assembly. J. Am. Chem. Soc. 122, 11547–11548.
Stojanovic, M.N., de Prada, P., Landry, D.W., 2001. Aptamer-based folding fluorescent sensor for cocaine. J. Am. Chem. Soc. 123, 4928–4931.
Stojanovic, M.N., Landry, D.W., 2002. Aptamer-based colorimetric probe for cocaine. J. Am. Chem. Soc. 124, 9678–9679.
Strano-Rossi, S., Molaioni, F., Rossi, F., Botrè, F., 2005. Rapid screening of drugs of abuse and their metabolites by gas chromatography/mass spectrometry: application to urinalysis. Rapid Commun. Mass Spectrom. 19, 1529–1535.
Swensen, J.S., Xiao, Y., Ferguson, B.S., Lubin, A.A., Lai, R.Y., Heeger, A.J., Plaxco, K.W., Soh, H.T., 2009. Continuous, real-time monitoring of cocaine in undiluted blood serum via a microfluidic, electrochemical aptamer-based sensor. J. Am. Chem. Soc. 131, 4262–4266.
Thompson, M., Ballantyne, S.M., Cheran, L.-E., Stevenson, A.C., Lowe, C.R., 2003. Electromagnetic excitation of high frequency acoustic waves and detection in the liquid phase. Analyst 128, 1048–1055.
Thompson, M., Blaszykowski, C., Sheikh, S., Romaschin, A., 2015. A true theranostic approach to medicine: towards tandem sensor detection and removal of endotoxin in blood. Biosens. Bioelectron. 67, 3–10.
Trachta, G., Schwarze, B., Sägmüller, B., Brehm, G., Schneider, S., 2004. Combination of high-performance liquid chromatography and SERS detection applied to the analysis of drugs in human blood and urine. J. Mol. Struct. 693, 175–185.
US Food and Drug Administration, 1996. Guidance for industry: Q2B validation of analytical procedures: methodology. Rockville, MD.
Wang, R., Li, Y., 2013. Hydrogel based QCM aptasensor for detection of avian influenza virus. Biosens. Bioelectron. 42, 148–155.
Wang, X., Ellis, J.S., Lyle, E.-L., Sundaram, P., Thompson, M., 2006. Conformational chemistry of surface-attached calmodulin detected by acoustic shear wave propagation. Mol. BioSyst. 2, 184–192.
Wen, Y., Pei, H., Wan, Y., Su, Y., Huang, Q., Song, S., Fan, C., 2011. DNA nanostructure-decorated surfaces for enhanced aptamer-target binding and electrochemical cocaine sensors. Anal. Chem. 83, 7418–7423.
White, R.J., Phares, N., Lubin, A.A., Xiao, Y., Plaxco, K.W., 2008. Optimization of electrochemical aptamer-based sensors via optimization of probe packing density and surface chemistry. Langmuir 24, 10513–10518.
Wu, A.H.B., McKay, C., Broussard, L.A., Hoffman, R.S., Kwong, T.C., Moyer, T.P., Otten, E.M., Welch, S.L., Wax, P., 2003. National academy of clinical biochemistry laboratory medicine practice guidelines: recommendations for the use of laboratory tests to support poisoned patients who present to the emergency department. Clin. Chem. 49, 357–379.
Xiao, Y., Piorek, B.D., Plaxco, K.W., Heeger, A.J., 2005. A reagentless signal-on architecture for electronic, aptamer-based sensors via target-induced strand displacement. J. Am. Chem. Soc. 127, 17990–17991.
Xie, S., Walton, S.P., 2009. Application and analysis of structure-switching aptamers for small molecule quantification. Anal. Chim. Acta 638, 213–219.
Yan, L., Zhu, Z., Zou, Y., Huang, Y., Liu, D., Jia, S., Xu, D., Wu, M., Zhou, Y., Zhou, S., Yang, C.J., 2013. Target-responsive “sweet” hydrogel with glucometer readout for portable and quantitative detection of non-glucose targets. J. Am. Chem. Soc. 135, 3748–3751.
Zhang, D.-W., Sun, C.-J., Zhang, F.-T., Xu, L., Zhou, Y.-L., Zhang, X.-X., 2012a. An electrochemical aptasensor based on enzyme linked aptamer assay. Biosens. Bioelectron. 31, 363–368.
Zhang, D.-W., Zhang, F.-T., Cui, Y.-R., Deng, Q.-P., Krause, S., Zhou, Y.-L., Zhang, X.-X., 2012b. A label-free aptasensor for the sensitive and specific detection of cocaine using supramolecular aptamer fragments/target complex by electrochemical impedance spectroscopy. Talanta 92, 65–71.
Zhang, J., Wang, L., Pan, D., Song, S., Boey, F.Y.C., Zhang, H., Fan, C., 2008. Visual cocaine detection with gold nanoparticles and rationally engineered aptamer structures. Small 4, 1196–1200.
Zhou, J., Ellis, A.V., Kobus, H., Voelcker, N.H., 2012. Aptamer sensor for cocaine using minor groove binder based energy transfer. Anal. Chim. Acta 719, 76–81.
Zhou, Z., Du, Y., Dong, S., 2011. DNA-Ag nanoclusters as fluorescence probe for turn-on aptamer sensor of small molecules. Biosens. Bioelectron. 28, 33–37.
Zuo, X., Xiao, Y., Plaxco, K.W., 2009. High specificity, electrochemical sandwich assays based on single aptamer sequences and suitable for the direct detection of small-molecule targets in blood and other complex matrices. J. Am. Chem. Soc. 131, 6944–6945.